Bulk-mediated surface diffusion: non-Markovian desorption and biased behaviour in an infinite system

2005 J. Phys.: Condens. Matter 17 S4175

(http://iopscience.iop.org/0953-8984/17/49/012)

INSTITUTE OF PHYSICS PUBLISHING JOURNAL OF PHYSICS: CONDENSED MATTER

J. Phys.: Condens. Matter **17** (2005) S4175–S4187 doi:10.1088/0953-8984/17/49/012

Bulk-mediated surface diffusion: non-Markovian desorption and biased behaviour in an infinite system

Jorge A Revelli[1], **Carlos E Budde**[1] **and Horacio S Wio**[2,3,4]

[1] Facultad de Matemáticas, Astronomía y Física, Universidad Nacional de Córdoba, 5000 Córdoba, Argentina
[2] Instituto de Física de Cantabria, Universidad de Cantabria and CSIC, E-39005 Santander, Spain
[3] Centro Atómico Bariloche and Instituto Balseiro, 8400 Bariloche, Argentina

E-mail: wio@ifca.unican.es

Received 24 June 2005, in final form 28 September 2005
Published 25 November 2005
Online at stacks.iop.org/JPhysCM/17/S4175

Abstract

We analyse the dynamics of adsorbed molecules within the *bulk-mediated surface diffusion* framework. We consider that the particle's desorption mechanism is characterized by a non-Markovian process, while the particle's adsorption and its motion in the bulk are governed by Markovian dynamics, and include the effect of an external field in the form of a bias in the normal motion to the surface. We study this system for the diffusion of particles in a semi-infinite lattice, analysing the conditional probability to find the system on the reference absorptive plane as well as the surface dispersion as functions of time. The agreement between numerical and analytical asymptotic results is discussed.

1. Introduction

Since the pioneering works of Einstein, Smoluchovski and Langevin [1], the study of diffusion processes has pervaded all areas of sciences and technology. During the last few decades, the literature on diffusion processes has ranged from some formal mathematical aspects [2], through diffusion-limited reactions [3] and anomalous diffusion or diffusion in disordered systems [4], to heat conductivity in solids [5] as well as other diffusion problems in material science [6]. Even the description of some problems in cardiology, biology and sociology have found and adequate framework in the diffusion approach [7]. Among the many problems studied in material science, the dynamics of adsorbed molecules at an adsorbing surface is a fundamental issue in interface science and is crucial to a number of emerging technologies [8] (for instance, see [9–12] and references therein).

Recently, the mechanism called *bulk-mediated surface diffusion* has been identified and explored [13, 14]. The importance of bulk–surface exchange in relaxing homogeneous surface

[4] Author to whom any correspondence should be addressed.

density perturbations is experimentally well established [15–20]. This mechanism typically arises at interfaces separating a liquid bulk phase and a second phase which may be either solid, liquid, or gaseous. Whenever the adsorbed species are soluble in the liquid bulk, adsorption–desorption processes occur continuously. These processes generate surface displacement because desorbed molecules undergo Fickian diffusion in the liquid's bulk, and are latter re-adsorbed elsewhere. When this process is repeated many times, an effective diffusion results for the molecules on the surface. Recent experiments [21] have demonstrated that the hydrodynamic flow has a strong effect on spin–lattice relaxation in water filled into a porous monolithic silica material. This is a rotational analogue of the translational hydrodynamic dispersion arising from incoherent Brownian motion in combination with coherent (or biased) flow. These results directly verify bulk-mediated surface diffusion, revealing in this way interfacial slip at fluid–solid interfaces.

Usually the studies performed in this type of system are done within the framework of a master equation scheme [13, 14, 22], where the particle's motion through the bulk and the adsorption–desorption processes are Markovian. In a series of recent papers we have shown some of the most important features of this phenomenon [9–12]: in particular, by studying the variance $\langle r^2(t)\rangle_{\text{plane}}$ of the position $\vec{r} \equiv (x, y)$ on the interface, or the conditional probability $P(z = 1, t) \equiv \sum_{x,y} P(x, y, z = 1; t|0, 0, 1; t = 0)$ to find the particle on the interface at time t, if it was initially at (0, 0, 1), through both analytical and numerical methods; the following results were obtained. For the case of a semi-infinite or unbounded bulk [9]

- for $t \to \infty$, the effective diffusion on the interface (first layer of the lattice) is always *sub-diffusive* (the variance of the position grows as $t^{1/2}$) *regardless* of the desorption rate δ. Similarly, the probability to find the particle on the interface at time t decays as $t^{-1/2}$, independently of δ;
- at *finite* times, the growth of the variance can be fitted by a t^{ϵ} law. The exponent ϵ depends on the range of time considered and the values of the adsorption and diffusion constants, increasing rapidly as δ decreases and saturating at a value compatible with the one reported in [13, 14];
- an effective *continuous-time random walk* (CTRW) description (*without conservation of probability*) was derived *on the interface*.

For the finite or bounded bulk case [10], we have investigated the transition from a multilayered to unbounded bulk regime, and found that

- there exists an optimal number of layers that maximizes $\langle r^2(t)\rangle_{\text{plane}}$ on the interface (which is a measure of the effective diffusivity);
- and up to about that thickness, the long time effective diffusivity on the interface has *normal* character, and crosses over abruptly towards a sub-diffusive behaviour as the number of layers increases further.

It is worth remarking here that for an arbitrary (finite) number of layers, the Laplace transform usually cannot be analytically inverted. This forced us to apply numerical inversion methods whose efficacy has been tested—with excellent results—not only against analytically solvable cases, like the bilayer one, but also against Monte Carlo simulations.

For the finite and infinite bulk cases, we have also investigated the situation when the particle's desorption is characterized by a non-Markovian process, while the particle's adsorption and its motion in the bulk are governed by a Markovian dynamics. We have found that [11, 12]

- for any non-Markovian desorption waiting time density with a *finite first moment*, the long time behaviour of both $\langle r^2(t)\rangle_{\text{plane}}$ and $P(z=1,t)$ is the same as in the Markovian case and only depends on the first moment of the waiting time function $\psi(t)$;
- for some class of non-Markovian desorption waiting time densities, in the 'strong adsorption' limit, there are two regimes: a transient and a stationary one. The main feature of the transient regime is that it is characterized by damped oscillations whose frequencies are in direct relation to the average desorption rate. Such an oscillatory effect disappear in the 'weak adsorption' region;
- it was analytically shown that, when the waiting time density for desorption has an *infinite* first moment, an asymptotic *sub-diffusive* regime appears for all values of ν (a parameter that characterizes the behaviour of the 'tail' of $\psi(t)$, $0<\nu<1$), except for $\nu=\frac{1}{2}$ where *normal diffusion* takes place.

In this work we address the dynamics of adsorbed molecules when, in addition to the particle's desorption mechanism being characterized by a non-Markovian process, while the particle's adsorption and its motion in the bulk are governed by a Markovian dynamics, there is a biased behaviour for the motion along the vertical axis (that is, we consider the effect of some external field normal to the interface). Diffusion in the presence of a biasing field is of great interest in several areas such as positron tomography [23], where the addition of a strong electric field perpendicular to the surface leads to greater sample penetration, the analysis of wetting layer growth under the action of a uniform gravitational field [24], particle segregation due to shaking in a gravitational field [25], and the steady-state regime due to a small field in two-dimensional diffusing reactants [26].

As is well known, a non-Markovian desorption process can occur when the surface contains 'deep traps', capture and re-emission from a surface that contains sites with several internal states such as the 'ladder trapping model', proteins with active sites deep inside its matrix, etc [27, 28]. It is worth remarking that, when non-Markovian process are present, it is necessary to resort to *generalized master equations*. These equations are characterized by a 'memory kernel' and may be related univocally with a CTRW scheme (for instance, see the paper by Montroll in [2]).

The main goal of this work is to study the influence of both the non-Markovian desorption and the indicated biased dynamics on the effective diffusion process at the interface $z=1$. For that purpose we calculate the temporal evolutions of the variance ($\langle r^2(t)\rangle_{\text{plane}}$) and $P(z=1,t)$, which (as indicated above) is the conditional probability of finding the particle on the surface at time t since the particle arrived there at $t=0$.

In the next section we formally present the model, in terms of a generalized master equation which describes the particle's dynamics through the bulk and surface, and its desorption. We indicate the differences that are introduced into the formalism by the non-Markovian desorption process and the biased behaviour. In the following section we discuss the asymptotic behaviour when the waiting time density has a long or a short time tail. After that, we present some numerical results for the non-Markovian desorption and biased case for infinite systems when the memory function has both short or long time tails. Finally, in the last section we discuss the results and present some conclusions.

2. The adsorption–desorption model: simultaneous non-Markovian and biased case

Here we consider the case of non-Markovian desorption. We use the same framework as in [11, 12]. Now $P(n,m,l;t)$ satisfies the following generalized master equation:

$$\dot{P}(n,m,1;t)=\gamma_1 P(n,m,2;t)-\int_0^t \mathrm{d}t'\,K(t')P(n,m,1;t-t'),$$

$$
\begin{aligned}
&+\alpha_1[P(n-1,m,1;t)+P(n+1,m,1;t)-2P(n,m,1;t)]\\
&+\beta_1[P(n,m-1,1;t)+P(n,m+1,1;t)-2P(n,m,1;t)], \qquad \text{for } l=1\\
\dot{P}(n,m,2;t) &= \int_0^t \mathrm{d}t'\, K(t')P(n,m,1;t-t')\\
&+\gamma_1 P(n,m,3;t)-\gamma_2 P(n,m,2;t)-\gamma_1 P(n,m,2;t)\\
&+\alpha[P(n-1,m,2;t)+P(n+1,m,2;t)-2P(n,m,2;t)]\\
&+\beta[P(n,m-1,2;t)+P(n,m+1,2;t)-2P(n,m,2;t)], \qquad \text{for } l=2\\
\dot{P}(n,m,l;t) &= \alpha[P(n-1,m,l;t)+P(n+1,m,l;t)-2P(n,m,l;t)]\\
&+\beta[P(n,m-1,l;t)+P(n,m+1,l;t)-2P(n,m,l;t)]\\
&+\gamma_1[P(n,m,l+1;t)-P(n,m,l;t)]+\gamma_2[P(n,m,l-1;t)\\
&-P(n,m,l;t)], \qquad \text{for } l\geqslant 3
\end{aligned}
\tag{1}
$$

where α and β are the transition probabilities per unit time through the bulk in the x, y directions respectively, while γ_1 and γ_2 are the transition probabilities per unit time through the bulk in the z direction that, when $\gamma_1 \neq \gamma_2$, indicates a biased behaviour (or the presence of an external field). It is important to note that the model presented in equation (1) allows for the possibility that the particles can move in the plane $z=1$ with temporal frequencies α_1 in the x direction and β_1 in the y direction. If these temporal frequencies are equal to zero, the motion through the $z=1$ plane is exclusively due to the dynamics across the bulk. $K(t)$ represents the memory kernel for desorption at all sites over the $z=1$ surface (that is for $(n,m,l=1)$). It is clear that when $\gamma_1=\gamma_2=\gamma$ (and $\alpha_1=\beta_1=0$), we recover the same set of equations used in [11, 12]. Also, if in addition we have that $K(t)\to\delta\delta(t)$, where $\delta(t)$ is the Dirac delta function, the system of Markovian equations used in [9, 10] is recovered.

Taking the Fourier transform with respect to the x and y variables and the Laplace transform with respect to the time t in the above equations, we obtain

$$
\begin{aligned}
&sG(k_x,k_y,1;s)-P(k_x,k_y,1,t=0)=\gamma_1 G(k_x,k_y,2;s)+A_1(k_x,k_y)G(k_x,k_y,1;s)\\
&\qquad -K(s)G(k_x,k_y,1;s), \qquad \text{for } l=1\\
&sG(k_x,k_y,2;s)-P(k_x,k_y,2,t=0)=A(k_x,k_y)G(k_x,k_y,2;s)+K(s)G(k_x,k_y,1;s)\\
&\qquad -\gamma_1 G(k_x,k_y,2;s)+\gamma_1 G(k_x,k_y,3;s)-\gamma_2 G(k_x,k_y,2;s), \qquad \text{for } l=2\\
&sG(k_x,k_y,l;s)-P(k_x,k_y,l,t=0)=A(k_x,k_y)G(k_x,k_y,l;s)+\gamma_1[G(k_x,k_y,l-1;s)\\
&\qquad -G(k_x,k_y,l;s)]+\gamma_2[G(k_x,k_y,l+1;s)-G(k_x,k_y,l;s)], \qquad \text{for } l\geqslant 3.
\end{aligned}
\tag{2}
$$

Here we have used the same definitions as in [9–12]. In particular we have

$$A(k_x,k_y)=2\alpha[\cos(k_x)-1]+2\beta[\cos(k_y)-1],$$

and

$$A_1(k_x,k_y)=2\alpha_1[\cos(k_x)-1]+2\beta_1[\cos(k_y)-1].$$

Clearly, the above equations for $G(k_x,k_y,l;s)]$ are similar to equation (2) in [10], with $K(s)$ instead of δ, and the unbiased γ replaced by γ_1 and γ_2. Therefore all results obtained in [9, 10] remain valid for a non-Markovian dynamics when δ is replaced by $K(s)$, and the bias is adequately included. Namely, the Laplace transform of the variance $\langle r^2(s)\rangle_{\text{plane}}=\mathcal{L}[\langle r^2(t)\rangle_{\text{plane}}]$ can be found as [9–12]

$$\langle r^2(s)\rangle_{\text{plane}}=-\left[\frac{\partial^2}{\partial k_x^2}+\frac{\partial^2}{\partial k_y^2}\right][\tilde{G}_{11}]\Big|_{k_x=k_y=0}. \tag{3}$$

In what follows, and in order to simplify and to focus on the joint effect of both the non-Markovian desorption and the bias, we adopt $\alpha = \beta$ and $\alpha_1 = \beta_1$ (we will finally consider the case $\alpha_1 = \beta_1 = 0$).

By using equations (3) and (12) of [10], $\langle r^2(s)\rangle_{\text{plane}}$ turns out to be the ratio of two complicated functions of s:

$$\langle r^2(s)\rangle_{\text{plane}} = \frac{N(s)}{D(s)}, \tag{4}$$

where

$$\begin{aligned} N(s) = {} & (8\alpha K(s)\gamma_1)\Big(\gamma_1^3 + \gamma_2^3 + s^3 + 3\gamma_1^2 s + 3\gamma_2^2 s + 3\gamma_1\gamma_2 s \\ & + 3\gamma_1 s^2 + 3\gamma_2 s^2 - \sqrt{(\gamma_1+\gamma_2+s)^2 - 4\gamma_1\gamma_2}\,\left(\gamma_1^2 + (\gamma_2+s)^2 + \gamma_1(\gamma_2+2s)\right)\Big) \\ & + (8\alpha_1\gamma_1\gamma_2)\Big(\sqrt{(\gamma_1+\gamma_2+s)^2 - 4\gamma_1\gamma_2}\,\left(\gamma_1^2 + 2\gamma_1 s + (\gamma_2+s)^2\right) \\ & - (\gamma_1+\gamma_2+s)((\gamma_1-\gamma_2)^2 + 2(\gamma_1+\gamma_2)\,s + s^2)\Big), \end{aligned} \tag{5}$$

and

$$\begin{aligned} D(s) = {} & \sqrt{(\gamma_1+\gamma_2+s)^2 - 4\gamma_1\gamma_2}\Bigg\{\sqrt{\frac{\gamma_1}{\gamma_2}}\Bigg((\gamma_2 - K(s))(\gamma_1^2 + 2\gamma_1 s + (\gamma_2+s)^2) \\ & - \sqrt{(\gamma_1+\gamma_2+s)^2 - 4\gamma_1\gamma_2}(\gamma_2 - K(s))(\gamma_1+\gamma_2+s)\Bigg) \\ & + \sqrt{\gamma_1\gamma_2}\Bigg(\sqrt{(\gamma_1+\gamma_2+s)^2 - 4\gamma_1\gamma_2}(\gamma_1+\gamma_2-K(s)) \\ & - (\gamma_1^2 + (\gamma_2 - K(s))(\gamma_2+s)) + \gamma_1(s - K(s))\Bigg)\Bigg\}^2. \end{aligned} \tag{6}$$

For $P(z=1,t)$, according to the result shown in [9], we have

$$\tilde{P}(z=1,s) = 2\gamma_1\gamma_2\Big(2\gamma_1\gamma_2 s + K(s)\Big[\gamma_1\gamma_2 + \gamma_1\Big(\sqrt{(\gamma_1+\gamma_2+s)^2 - 4\gamma_1\gamma_2} - s - \gamma_1\Big)\Big]\Big)^{-1}. \tag{7}$$

We reiterate that, as indicated in [9], the conservation of particles on the plane is not satisfied. Also, the relation between $\psi(t)$, the waiting time density, as defined in a CTRW scheme, and the memory kernel of equation (1), in the Laplace domain reads [2] $K(s) = s\psi(s)\{1-\psi(s)\}^{-1}$.

3. Asymptotic behaviour

Here we show the results, obtained via Tauberian theorems [29], about the asymptotic long time system's behaviour in two cases: when the waiting time function has a short or a long time tail. We assume that, when $s \ll 1$, $\psi(s) \sim 1 - Bs^\nu$ with $0 < \nu < 1$ for the case of a *long tail*, and $\nu = 1$ for the *short tail* case. In the case of short tail waiting time densities we have $B = \langle t\rangle_{\text{ads}}$. Consequently, in this limit $K(s) \sim \frac{1}{B}s^{1-\nu}$. In this expression we still retain the diffusion contribution on the surface (that is, we still keep that $\alpha_1 = \beta_1 \neq 0$).

Considering the different possibilities we have three cases: (i) $\boldsymbol{\gamma_1 > \gamma_2}$; (ii) $\boldsymbol{\gamma_1 < \gamma_2}$; and (iii) $\boldsymbol{\gamma_1 = \gamma_2 = \gamma}$.

3.1. Short tail

- $\gamma_1 > \gamma_2$

$$\langle r^2(t)\rangle_{\text{plane}} \sim \left(\frac{4(\gamma_1-\gamma_2)}{(\gamma_1-\gamma_2+\frac{1}{B})^2}\left(\frac{\alpha}{B}+\alpha_1(\gamma_1-\gamma_2)\right)\right)t, \tag{8}$$

and

$$P(z=1,t) \sim \left\{1+\frac{1}{B(\gamma_1-\gamma_2)}\right\}^{-1} \tag{9}$$

- $\gamma_1 < \gamma_2$. In this case, both $\langle r^2(t)\rangle_{\text{plane}}$ and $P(z=1,t)$ show an exponential decay.
- $\gamma_1 = \gamma_2 = \gamma$

$$\langle r^2(t)\rangle_{\text{plane}} \sim 4\,B\,\alpha\,\left(\frac{\gamma}{\pi}\right)^{\frac{1}{2}}\,t^{\frac{1}{2}}, \tag{10}$$

and

$$P(z=1,t) \sim B\,\left(\frac{\gamma}{\pi}\right)^{\frac{1}{2}}\,t^{-\frac{1}{2}}. \tag{11}$$

The above results are the expected ones for a short tail case. Clearly, for $\gamma_1 < \gamma_2 = \gamma$, the $P(z=1,t)$ decays to zero (exponentially), while for $\gamma_1 = \gamma_2$ it also decays, but much more slowly (potentially).

3.2. Long tail

- $\gamma_1 > \gamma_2$

$$\langle r^2(t)\rangle_{\text{plane}} \sim \frac{4\,\alpha_1(\gamma_1-\gamma_2)^2}{\gamma_2^2}\,t + 4\alpha\frac{(\gamma_1-\gamma_2)}{B\gamma_2^2\,\Gamma(1+\nu)}\,t^{\nu}, \tag{12}$$

and

$$P(z=1,t) \sim 1. \tag{13}$$

- $\gamma_1 < \gamma_2$

$$\langle r^2(t)\rangle_{\text{plane}} \sim \frac{4\,(B\,\gamma_2)^2\,\alpha_1}{(\gamma_1-\gamma_2)^2\,\Gamma(2(1-\nu))}\,t^{1-2\nu} + 4\,B\,\frac{\gamma_1\,\gamma_2\,\alpha}{(\gamma_1-\gamma_2)^3\Gamma(1-\nu)}\,t^{-\nu}, \tag{14}$$

and

$$P(z=1,t) \sim \frac{B\gamma_2}{\Gamma(1-\nu)(\gamma_2-\gamma_1)}t^{-\nu}. \tag{15}$$

- $\gamma_1 = \gamma_2 = \gamma$. Here we have different asymptotic behaviours depending on the range of values of ν.

$$\langle r^2(t)\rangle_{\text{plane}} \sim \begin{cases} \dfrac{(2\alpha)}{B\sqrt{\gamma}\Gamma(\frac{3}{2}+\nu)}t^{\frac{1}{2}+\nu} + 4\,\alpha_1\,t, & 0<\nu<\frac{1}{2} \\ \dfrac{(2\alpha)B\sqrt{\gamma}+4\,\gamma\,B^2\alpha_1}{(B\sqrt{\gamma}+1)^2}\,t & \nu=\frac{1}{2} \\ \dfrac{4\gamma\,B^2\alpha_1}{\Gamma(3-2\nu)}\,t^{2(1-\nu)} + 2\,\dfrac{\alpha\,B\sqrt{\gamma}}{\Gamma(\frac{5}{2}-\nu)}\,t^{\frac{1}{2}-\nu} & \frac{1}{2}<\nu<1 \end{cases} \tag{16}$$

and

$$P(z=1,t) \sim \begin{cases} 1, & 0 < \nu < \frac{1}{2} \\ \dfrac{B\sqrt{\gamma}}{(B\sqrt{\gamma}+1)}, & \nu = \frac{1}{2} \\ \dfrac{B\sqrt{\gamma}}{\Gamma(\frac{1}{2}-\nu)} t^{\frac{1}{2}-\nu}, & \frac{1}{2} < \nu < 1. \end{cases} \tag{17}$$

From equation (16) it can be deduced that an asymptotic *sub-diffusive* regime arises for all values of ν ($0 < \nu < 1$) except in the case $\nu = \frac{1}{2}$, where *normal diffusion* takes place. As in [12], this occurs due to the 'competition' between adsorption and Fickian diffusion across the bulk. We have shown in [9] that the probability density to return for the first time to the plane $z = 1$ is proportional to $t^{-\frac{3}{2}}$ for large times; it is the behaviour of the desorption waiting time density function with $\nu = \frac{1}{2}$ that produces the particular value of this parameter. The ladder trapping model [27] with infinite number of internal states is an important example where the desorption waiting time density is characterize by a parameter $\nu = \frac{1}{2}$.

The above-indicated asymptotic behaviour, for both short and long time tails in the waiting time function, in addition to its intrinsic value, will help us to understand some of the numerical results to be shown in the following section.

4. Numerical results: Laplace transform

In this section we show the results obtained numerically. As was discussed in previous works [9, 10], for general cases, the Laplace transform of $\langle r^2(s)\rangle_{\text{plane}}$ and $P(z=1,s)$ usually cannot be analytically inverted. This occurs in the present case; hence we have been forced to employ a numerical inversion method. The efficacy of such a method was established in [9, 10], where it was shown that it is a reliable tool and that we can trust their results in those cases where analytical results are not accessible [30]. In all cases, and in order to focus on the competition between non-Markovian desorption and the bias, we have adopted $\alpha_1 = \beta_1 = 0$.

To describe the desorption dynamics from the surface we have used two families of waiting time densities ($\psi(t)$). The first one, since it was first introduced by Scher and Lax [32] to describe the frequency dependence of the electric conductivity in disordered solids when transport is due to impurity hopping, has been extensively exploited in modelling non-Markovian situations (see also [29]). The reasons for its wide use are the versatile functional form and its simplicity that allows one to take into account a spread of transition rates in a controllable way [32]. When only one transition rate is present a Markovian description is reobtained: the memory kernel becomes a Dirac δ-function. The form is

$$\psi(t) = \theta a \frac{(\theta a t)^{(a-1)}}{\Gamma(a)} \mathrm{e}^{-\theta a t}, \tag{18}$$

where a is a positive integer and $\Gamma(a)$ is the Gamma or factorial function. It is worth remarking here two important facts about this family of functions. First, as can be seen from equation (18), there are two parameters which characterize the function. The parameter a, called the *Markovianicity parameter*, defines the degree of non-Markovianicity of the function ($a = 1$ corresponds to the Markovian case; $a \neq 1$ to the non-Markovian case), while the parameter θ is the 'average desorption rate'. Second, as shown in [31], the mean value of these waiting time densities is

$$\langle t \rangle = \int_0^\infty t\psi(t)\,\mathrm{d}t = \theta^{-1}, \tag{19}$$

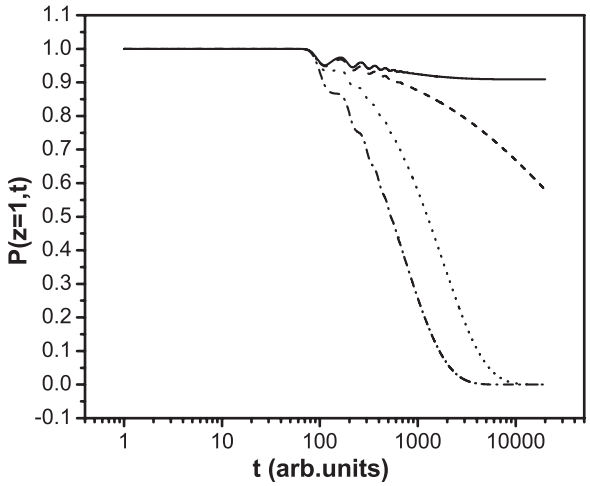

Figure 1. Temporal evolution of $P(z = 1, t)$, the probability distribution on the plane $z = 1$. Here we have adopted $\alpha = \beta = 1$, $\theta = 0.01$, $a = 50$ and $\gamma_1 = 1$. The different curves correspond, from top to bottom, to $\gamma_2 = 0.9$ (continuous line), $\gamma_2 = 1.0$ (dashed line), $\gamma_2 = 1.5$ (dotted line), $\gamma_2 = 5.0$ (dashed–dotted line).

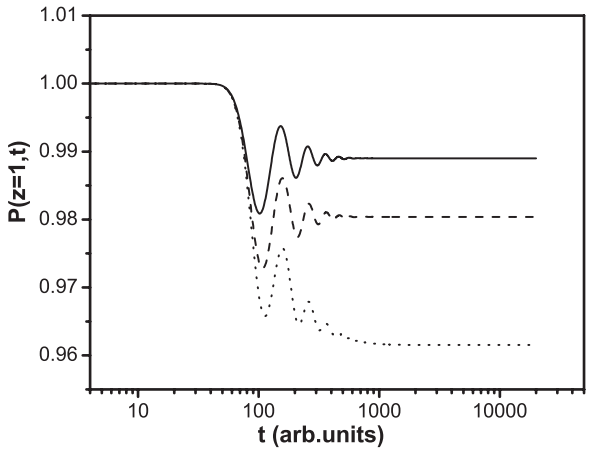

Figure 2. Temporal evolution of $P(z = 1, t)$, the probability distribution on the plane $z = 1$. We have adopted the same values of the parameters as in figure 1, except that $a = 20$. From top to bottom $\gamma_2 = 0.1$ (continuous line), $\gamma_2 = 0.5$ (dashed line), $\gamma_2 = 0.75$ (dotted line).

that is the 'average desorption time' does not depend on the a parameter, but is only function of the desorption rate. For the form of this family of functions, see figure 1 in [31].

Figures 1 and 2 show the dependence of $P(z = 1, t)$ for several cases. We have adopted $\alpha = \beta = 1$, $\theta = 0.01$ and $\gamma_2 = 1.0$. In figure 1 we have $a = 50$, and analyse what happens when γ_2 is varied. The long time behaviour is in clear agreement with the asymptotic results indicated in the previous section. In figure 2, we changed to $a = 20$, with similar results. The general behaviour is similar to the case without bias [12]. However, the departure from the unbiased behaviour when $\gamma_1 \neq \gamma_2$ is apparent.

In both figures there is apparent a (small) transient oscillatory behaviour, more marked in the second case. The origin of such oscillations has been explained in [12], and has been shown

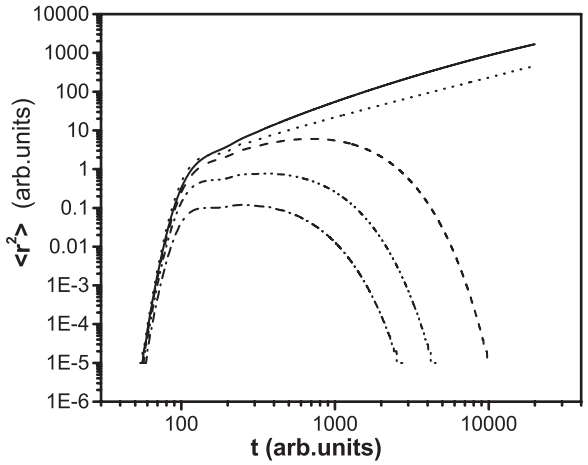

Figure 3. Temporal evolution of $\langle r^2(t)\rangle_{\text{plane}}$, the variance of the position $\vec{r} \equiv (x, y)$ on the plane $z = 1$. We have adopted $\alpha = \beta = 1$, $\theta = 0.01$, $a = 50$ and $\gamma_1 = 1$. From top to bottom $\gamma_2 = 0.2$ (continuous line), $\gamma_2 = 1.0$ (dotted line), $\gamma_2 = 1.5$ (dashed line), $\gamma_2 = 2.5$ (dashed–double dotted line), $\gamma_2 = 5.0$ (dashed–dotted line).

to be related with θ, the desorption rate. It was indicated that the oscillations only appear in the non-Markovian case and are due to the particular behaviour of the family of waiting time densities defined above. When the Markovianicity parameter tends to infinity, $a \to \infty$, it is well known that $\psi(t)$ tends towards a Dirac δ function: $\psi(t) \to \delta(t - \theta^{-1})$. This fact implies a kind of 'periodicity', as—on average—there is a desorption after each elapsed $\Delta t \simeq \theta^{-1}$ period.

In figure 3 we show the time dependence of the variance $\langle r^2(t)\rangle_{\text{plane}}$ for $\alpha = \beta = 1$, $\theta = 0.01$, $a = 50$ and $\gamma_1 = 1$, and different values of γ_2. The change from a growing variance for $\gamma_2 < \gamma_1$, until a receding variance for the opposite case $\gamma_2 > \gamma_1$ is apparent. Clearly, the change in behaviour occurs for $\gamma_2 = \gamma_1$. Again, the departure from the unbiased behaviour when $\gamma_1 \neq \gamma_2$ becomes apparent.

In order to analyse the long time tail case, we used a second family of desorption waiting time density functions that, defined in the Laplace domain [33], have the form

$$\psi(s) = \frac{1}{1 + (\frac{s}{\phi})^{\nu}}, \qquad 0 < \nu < 1. \tag{20}$$

However, as ϕ amounts to only a change in the timescale, we adopted $\phi = 1$. We have also fixed the parameters α, β, and γ_1, all equal to one.

In figure 4 we depict the dependence of $P(z = 1, t)$ for a long tail case, for a typical $\gamma_2 < \gamma_1$ case, with $\alpha = \beta = 1$, $\phi = 1$, $\gamma_1 = 1$ and $\gamma_2 = 0.8$, for different values of ν. The asymptotic behaviour determined in the previous section is clearly seen. It is interesting to remark on a receding behaviour before the increase towards the asymptotic behaviour, a fact that does not arise in the case without bias. In figure 5 we also depict the time dependence of $P(z = 1, t)$ for $\alpha = \beta = 1$, $\phi = 1$, $\gamma_1 = 1$ and $\nu = 0.1$, for different values of γ_2. Here also, the way that the asymptotic behaviour is reached becomes apparent. Figure 6 again shows the time dependence of $P(z = 1, t)$ for $\alpha = \beta = 1$, $\phi = 1$, $\gamma_1 = 1$ and $\nu = 0.5$, and different values of γ_2. The way the asymptotic behaviour is approached is clearly seen and, again, the departure from the unbiased behaviour when $\gamma_1 \neq \gamma_2$ becomes apparent.

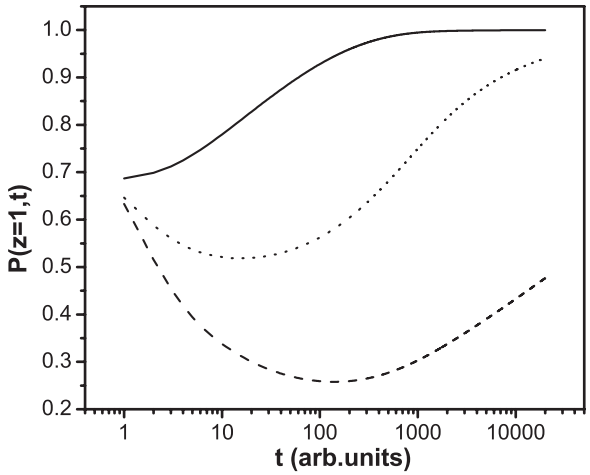

Figure 4. Temporal evolution of $P(z = 1, t)$. We have adopted $\alpha = \beta = 1$, $\phi = 1$, $\gamma_1 = 1$ and $\gamma_2 = 0.8$. The different curves correspond to $\nu = 0.1$ (continuous line), $\nu = 0.5$ (dotted line), $\nu = 0.75$ (dashed line).

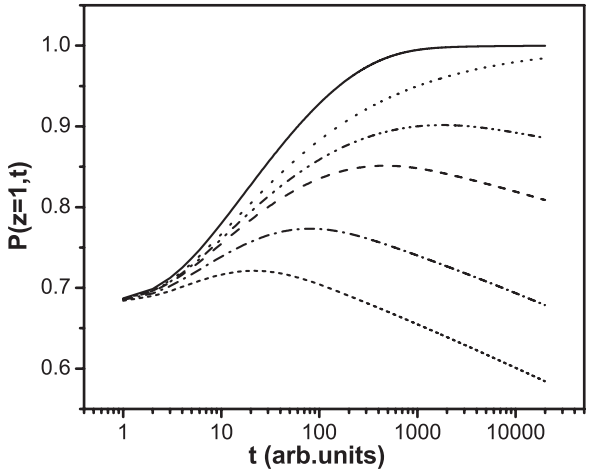

Figure 5. Temporal evolution of $P(z = 1, t)$. As in figure 4 we have adopted $\alpha = \beta = 1$, $\phi = 1$ and $\gamma_1 = 1$, while $\nu = 0.1$. From top to bottom $\gamma_2 = 0.8$ (continuous line), $\gamma_2 = 1.0$ (dotted line), $\gamma_2 = 1.1$ (dash–double dotted line), $\gamma_2 = 1.2$ (dashed line), $\gamma_2 = 1.5$ (dash–dotted line), $\gamma_2 = 2.$ (short-dashed line).

In figure 7, the time dependence of the variance $\langle r^2(t)\rangle_{\text{plane}}$ for $\alpha = \beta = 1$, $\phi = 1$, $\gamma_1 = 1$ and $\gamma_2 = 10$ and different values of ν is shown. The corresponding diffusive and sub-diffusive behaviour for the different values of ν is apparent. Finally, in figure 8 we show the time dependence of the variance $\langle r^2(t)\rangle_{\text{plane}}$ for $\alpha = \beta = 1$, $\phi = 1$, $\gamma_1 = 1$ and $\nu = 0.5$, for different values of γ_2. The collapse for $\gamma_2 > 1$ (that is for $\gamma_2 > \gamma_1$) is clearly seen.

5. Conclusions

We have studied the evolution of particles making an effective diffusion on a surface. The diffusion is actually performed both on the surface and across the bulk surrounding the surface,

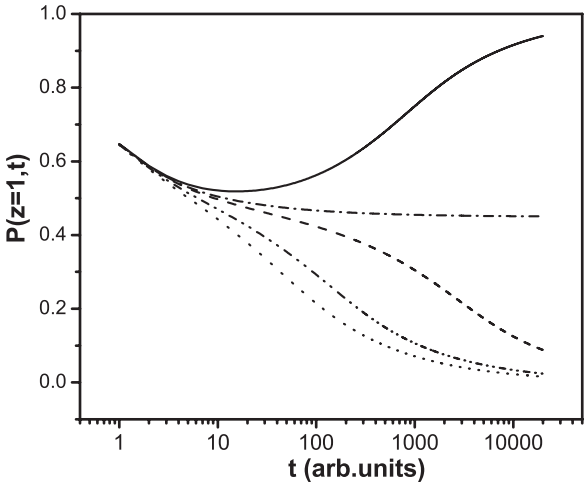

Figure 6. Temporal evolution of $P(z = 1, t)$. Here, as in figure 4, we have adopted $\alpha = \beta = 1$, $\phi = 1$ and $\gamma_1 = 1$, while $\nu = 0.5$. From top to bottom $\gamma_2 = 0.8$ (continuous line), $\gamma_2 = 1.0$ (dash–dotted line), $\gamma_2 = 1.1$ (dashed line), $\gamma_2 = 1.5$ (dash–double dotted line), $\gamma_2 = 2$ (dotted line).

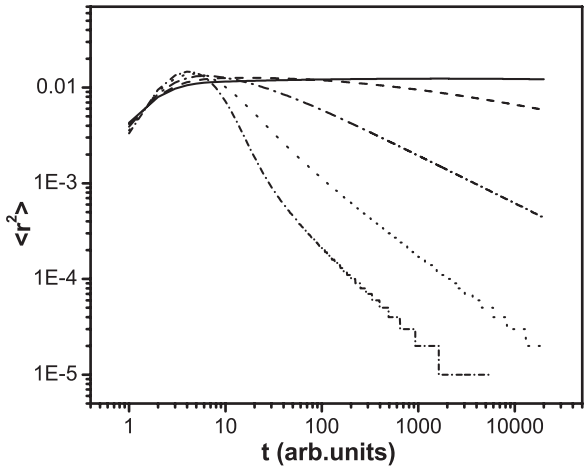

Figure 7. Temporal evolution of $\langle r^2(t)\rangle_{\text{plane}}$. We have adopted $\alpha = \beta = 1$, $\gamma_1 = 1$ and $\gamma_2 = 10$. From top to bottom $\nu = 0.1$ (continuous line), $\nu = 0.25$ (dashed line), $\nu = 0.5$ (dash–dotted line), $\nu = 0.75$ (dotted line), $\nu = 1.0$ (short dash–dotted line).

resulting in the so-called *bulk-mediated surface diffusion* phenomenon. The main feature of this work was to present an analytical model for non-Markovian desorption from the surface, also including the effect of an external (normal to the surface) field, through a biased behaviour in the normal direction. For the bulk that surrounds the surface we have considered that it is semi-infinite, and that the particles undergo a Markovian motion there.

We observed the influence of both effects on the effective diffusion process at the interface $z = 1$ by calculating analytically, in the Laplace domain, the temporal evolutions of $\langle r^2(t)\rangle_{\text{plane}}$, the variance, and $P(z = 1, t)$, the conditional probability of being on the surface at time t since the particle arrived there at $t = 0$. We have chosen two families of non-Markovian desorption

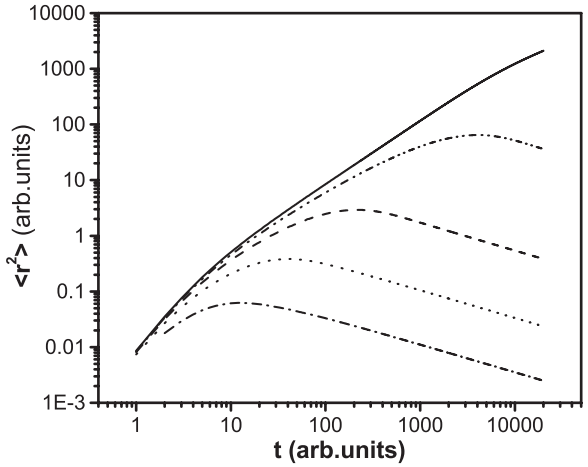

Figure 8. Temporal evolution of $\langle r^2(t)\rangle_{\text{plane}}$. We have adopted $\alpha = \beta = 1$, $\gamma_1 = 1$ and $\nu = 0.5$. From top to bottom $\gamma_2 = 0.9$ (continuous line), $\gamma_2 = 1.1$ (dash–double dotted line), $\gamma_2 = 1.5$ (dashed line), $\gamma_2 = 2.5$ (dotted line), $\gamma_2 = 5.0$ (dash–dotted line).

waiting time densities and analysed the numerical evaluation for $\langle r^2(t)\rangle_{\text{plane}}$ and $P(z = 1, t)$. One desorption waiting time density has a *finite first moment*, while the other corresponds to a waiting time density for desorption that has an *infinite* first moment. We have been able to deduce the asymptotic behaviour in both cases, determining regions of values of the parameter ν, obtaining asymptotic *sub-diffusive* regimes, or cases where *normal diffusion* takes place. However, from our analysis we have not obtained any kind of super-diffusive behaviour. The numerical results are in agreement with the indicated asymptotic ones.

Recent nuclear magnetic spin–lattice relaxation experiments [21] have been performed in partially filled porous glasses with wetting and non-wetting fluids. Basically they have demonstrated the existence of three mobility states of the fluid molecules: the adsorbed states at the pore walls, the bulk-like liquid phases and the vapour phase. The adsorbate spin lattice relaxation rate, usually denoted as the *reorientation mediated by translational displacements* (RMTD) mechanism, takes place at the adsorbate–matrix interface. The relaxation experimental data have been analysed in terms of *molecular exchanges* between the different mobility states. The spin–lattice relaxation rates allowed the authors to distinguish two limits, low and fast exchanges (relative to the RMTD timescale).

Finally, it is worth remarking here an important aspect of the present approach. Through the above results we have shown that the behaviour of $\langle r^2(t)\rangle_{\text{plane}}$ and of $P(z = 1, t)$ are strongly dependent on both the desorption mechanism and the effect of bias. As the effective dispersion and the percentage of particles that remain in $z = 1$ are measurable magnitudes [14], they may be used to investigate the characteristic and fundamental parameters of the desorption processes under the effect of a field. The present experimental techniques [21] are very sensitive and able to produce highly precise measurements of quantities directly related to those evaluated in the theory, like effective diffusivities, and in this way to test the theory.

Acknowledgments

CEB acknowledges partial support from ‘Agencia Cordoba Ciencia’, Argentina. HSW thanks the European Commission for the award of a Marie Curie Chair.

References

[1] Einstein A 1905 *Ann. Phys., Lpz.* **17** 549
Smoluchowski M V 1906 *Ann. Phys., Lpz.* **21** 756
Langevin P 1908 *Comp. Rendues* **146** 530
[2] Shlesinger M F and Weiss G H (ed) 1994 *The Wonderful World of Stochastics* (Amsterdam: North-Holland)
[3] Rice S A 1985 *Diffusion-Limited Reactions* (Amsterdam: Elsevier)
Ovchinnicov A A, Timashev S F and Belyy A A 1989 *Kinetics of Diffusion Controlled Chemical Physics* (Commack, NY: Nova Science)
[4] Bouchaud J P and Georges A 1990 *Phys. Rep.* **195** 127
[5] Carslaw H S and Jaeger J C 1959 *Conduction of Heat in Solids* (London: Oxford University Press)
[6] Doi M and Edwards S F 1986 *The Theory of Polymer Dynamics* (Oxford: Clarendon)
Fukai Y 1993 *The Metal–Hydrogen System* (Berlin: Springer)
[7] Jaliffe J (ed) 1990 Mathematical approaches to cardiac arrythmias *Ann. New York Acad. Sci.* **591**
Murray J D 1989 *Mathematical Biology* (Berlin: Springer)
Weidlich W 2002 *Sociodynamics—A Systematic Approach to Mathematical Modelling in Social Sciences* (London: Taylor and Francis)
[8] Clint J H 1992 *Surfactant Aggregation* (New York: Chapman and Hall)
[9] Revelli J A, Budde C E, Prato D and Wio H S 2003 *Eur. Phys. J.* B **36** 245–51
[10] Revelli J A, Budde C E, Prato D and Wio H S 2004 *Eur. Phys. J.* B **37** 205
[11] Revelli J A, Budde C E, Prato D and Wio H S 2005 *Eur. Phys. J.* B **43** 65
[12] Revelli J A, Budde C E, Prato D and Wio H S 2005 *New J. Phys.* **7** 16 (http://stacks.iop.org/1367-2630/7/16)
[13] Bychuk O V and O'Shaughnessy B 1995 *Phys. Rev. Lett.* **74** 1795
[14] Bychuk O and O'Shaughnessy B 1994 *J. Chem. Phys.* **101** 772
Stapf S, Kimmich R and Seitter R O 1995 *Phys. Rev. Lett.* **75** 2855
[15] Shibata C T and Lenhof A M 1992 *J. Colloid Interface Sci.* **148** 469
Shibata C T and Lenhof A M 1992 *J. Colloid Interface Sci.* **148** 485
[16] Levich V G 1962 *Physiochemical Hydrodynamics* 2nd edn (Englewood Cliffs, NJ: Prentice-Hall)
[17] Lucassen-Reynders E H and Lucassen J 1969 *Adv. Colloid Interface Sci.* **2** 347
[18] Lucassen-Reynders E H, Lucassen J, Garret P R, Giles D and Hollway F 1975 *Adv. Chem. Scr.* **144** 272
[19] Lin S-Y, McKeigue K and Maldarelli C 1990 *AIChE J.* **36** 1785
[20] Coppey M, Bénichou O, Klafter J, Moreau M and Oshanin G 2004 *Phys. Rev.* E **69** 036115
[21] Mattea C, Kimmich R, Ardelean I, Wonorohardjo S and Farrher G 2004 *J. Chem. Phys.* **121** 10648
Mattea C and Kimmich R 2005 *Phys. Rev. Lett.* **94** 024502
[22] van Kampen N G 1993 *Stochastic Processes in Physics and Chemistry* 2nd edn (Amsterdam: North-Holland)
[23] Schultz P J and Lynn K G 1988 *Rev. Mod. Phys.* **60** 701
[24] Pak H K and Law B M 1995 *Europhys. Lett.* **31** 19
[25] Alexander F J and Lebowitz J L 1994 *J. Phys. A: Math. Gen.* **27** 683
[26] Sibona G J, Budde C E and Condat C A 1996 *Phys. Rev.* E **54** 6232
[27] Haus J W and Kehr K W 1987 *Phys. Rep.* **150** 265
[28] Re M A and Budde C E 2000 *Phys. Rev.* E **61** 1110
[29] Montroll E W and West B J 1979 *Fluctuation Phenomena* ed E W Montroll and J L Lebowitz (Amsterdam: North-Holland)
[30] Honig G and Hirdes U 1980 *On the Application of an Efficient Algorithm for the Numerical Laplace Inversion* Kernforschungsanlage Jülich GmbH, Institut für Festkörperforschung
Revelli J A 2003 *PhD Thesis* Instituto Balseiro, Universidad Nacional de Cuyo, Argentina
[31] Revelli J A, Budde C E and Wio H S 2002 *Phys. Lett.* A **306** 104
[32] Scher H and Lax M 1973 *Phys. Rev.* B **7** 4491
Scher H and Lax M 1973 *Phys. Rev.* B **7** 4502
[33] Weiss G H 1966 *Adv. Chem. Phys.* **13** 1
Weiss G H 1994 *Aspects and Applications of the Random Walk* (Amsterdam: North-Holland)